Liu, W., Long, Z., and Chen, Q. 2012. "A procedure for predicting pressure loss coefficients of duct fittings using CFD (RP-1493)" HVAC&R Research, *18(6), 1168–1181*.

A procedure for predicting pressure loss coefficients of duct fittings using CFD (RP-1493)

Wei Liu,[1] Zhengwei Long,[1,*] Qingyan Chen[1,2]

[1] *School of Environmental Science and Engineering, Tianjin University, Tianjin 300072, China*
[2] *School of Mechanical Engineering, Purdue University, West Lafayette, IN 47907, USA*
** Correspondence author. E-mail: longzw@tju.edu.cn*

Knowing loss coefficients of duct fittings is crucial for designing a duct network for HVAC systems. Traditionally, the coefficients have been obtained using experimental measurements according to AHSRAE Standard 120, a process which is time consuming and expensive. An alternative is to use CFD, but this has uncertainty due to the approximations used in modeling turbulence. This study first validated three turbulence models by comparing the predicted loss coefficient of an elbow with the corresponding experimental data from the literature. The Standard k-ε model and Reynolds stress model could accurately predict the loss coefficient; however, the more advanced LES model failed. The study found that the surface roughness of the straight duct connected to the elbow had a significant influence on the predicted pressure loss and that the accurate surface roughness could be determined. Then, this study applied the same procedure and turbulence models to predict the pressure loss coefficient of a lateral and a tee junction with both converging and diverging flows. The results show again that the surface roughness of the straight duct connected to the junctions was very important and that the best value could be estimated. The pressure loss coefficients predicted were accurate when compared with the experimental data available to us after the simulations. Some discrepancies between the calculated and measured results exist that could be attributed to the approximations used in the simulations or the errors in the experimental measurements.

Introduction

Heating, Ventilation, and Air-conditioning (HVAC) systems in buildings and other enclosed spaces are crucial for creating a comfortable and healthy indoor environment. These HVAC systems always require duct systems to deliver air. To increase the energy efficiency of the fans in HVAC systems, the pressure loss of the duct network should be minimized, which would require accurate estimation of the pressure loss coefficient of the duct fittings.

The existing design guides for duct systems do not include many of the duct fittings used in HVAC systems. This compels designers to make intelligent guesses for some of the pressure loss coefficients used in their calculations (Shao et al. 1995). ASHRAE Standard 120 provides a standard experimental method of testing to determine the flow resistance of HVAC ducts and fittings. Kulkarni et al. (2009) measured the pressure loss coefficients of flat oval elbows with various aspect ratios. The experimental measurements could be accurate, but they are expensive and time-consuming.

Due to the development of computer speed and capacity and the improvements in turbulence modeling, Computational Fluid Dynamics (CFD) offers a fast and accurate alternative for obtaining the pressure loss coefficients of duct fittings. Shao et al. (1995) predicted pressure loss of double elbows using CFD and were able to achieve a relative error of about 10% using the k-ε model and the higher order QUICK scheme. Gan et al. (1995) determined numerically the loss coefficient of a square duct with bends, and they found that optimal predictions could be achieved using CFD with the standard k-ε model and quadratic upstream interpolation scheme. Gan et al. (1997) further studied the pressure loss of a square-edged orifice and perforated plates by CFD and found reasonably accurate results. Ahmet et al. (2007) also applied CFD to predict the pressure loss of compressed flexible ducts, and the CFD simulation results showed close proximity to laboratory experiments for fully stretched and 30% compressed flexible ducts. Mumma et al. (1997) conducted both a numerical and an experimental study of the coupled ductwork pressure drop. The close coupling condition resulted in an approximately 27% higher pressure loss of measured results than the predicted results with the Renormalized Group (RNG) k-ε model. Mahank and Mumma (1997) also applied a k-ε model to predict the pressure loss of a flat oval ductwork and compared

Wei Liu, Student Member ASHRAE, is graduate research assistant. **Zhengwei Long, PhD**, is lecturer. **Qingyan Chen, PhD**, Fellow ASHRAE, is Changjiang Chair Professor and Vicent P. Reilly Professor.

the predicted results with the measured data. Their study concluded that CFD methods may be efficiently and accurately used to analytically determine ductwork loss coefficients. However, when Mumma et al. (1998) applied the standard k-ε model to calculate the loss coefficient of nine different ductwork fittings, their predictions showed notable discrepancies among the experimental data for some cases. The above literature review concluded that CFD could be used to accurately predict the pressure loss coefficients of duct fittings, but the performance of CFD was not stable. Many studies have to tune their models with experimental data, which makes CFD less attractive.

The question is, if one does not have experimental data to validate the CFD model, could the CFD results still be trusted? ASHRAE Technical Committee 5.2 on "Duct Design" organized an international competition to encourage the CFD community to devise solutions to predict pressure loss coefficients of duct fittings without knowing the experimental data. The competition came about through ASHRAE Research Project 1493, "CFD Shootout Contest – Prediction of Duct Fitting Losses." The primary objectives of the contest were (1) to gain confidence in the use of CFD to determine the loss coefficients for duct fittings and (2) to eliminate laboratory fitting tests in compliance with ASHRAE Standard 120. Our team participated in the competition and won first prize. This paper reports on how our team simulated the pressure loss coefficients for the duct fittings provided by ASHRAE Research Project 1493 and how the results compared with the experimental data that were presented to us after we delivered the computed results to ASHRAE. The comparison presented here was without any modifications on the CFD simulations after we received the experimental data from ASHRAE Project Monitoring Subcommittee 1493.

Method

Governing Equations for CFD. This investigation used CFD to model the flow and pressure distributions of the duct fittings. Previous researchers (Gan et al. 1995; Gan et al. 1997; Ahmet et al. 2007) used the standard k-ε model (Launder and Spalding 1974) and a Reynolds stress model (RSM) (Gibson and Launder 1978) and showed some good results. Thus, this investigation used these models. In addition, Large Eddy Simulation (LES) (Germano et al. 1996) uses only one empirical coefficient in the model and is theoretically more accurate than the other two models. Therefore, this study used LES as well, so we had a total of three models. All these turbulence model equations can be written in a general form as:

$$\rho\frac{\partial\bar{\phi}}{\partial t}+\rho\bar{u}_j\frac{\partial\bar{\phi}}{\partial x_j}-\frac{\partial}{\partial x_j}\left[\Gamma_{\phi,eff}\frac{\partial\bar{\phi}}{\partial x_j}\right]=S_\phi \tag{1}$$

where ϕ represents variables, $\Gamma_{\phi,eff}$ the effective diffusion coefficient, S_ϕ the source term of the variable, ρ the fluid density, u_j the velocity component in the j direction, and x_j the coordinate in the j direction. As these models are available in commercial CFD software ANSYS FLUENT (2009), it was used for the present study.

Numerical Method. For the standard k-ε and RSM models, the SIMPLE algorithm was adopted to couple pressure and momentum equations. The standard scheme was used for pressure equation discretization, and the QUICK scheme for momentum equation discretization. This study used the first-order upwind scheme for all the other variables. The solutions were considered to be converged when the sum of the normalized residuals for all the cells became less than 10^{-5} for the variables:

$$R^\phi=\frac{\sum_{cellsP}\left|\sum_{nb}a_{nb}\phi_{nb}+b-a_P\phi_P\right|}{\sum_{cellsP}\left|a_P\phi_P\right|} \tag{2}$$

where, ϕ_P and ϕ_{nb} are the variable of the present and neighboring cells, respectively, a_P is the coefficient of the present cell, a_{nb} are the coefficients for the neighboring cells, and b is the contribution of the constant part of the source term and boundary conditions. This investigation solved only steady-state equations for the standard k-ε and RSM models. For LES, the algorithm, discretization schemes, and convergence criteria were the same as those for the standard k-ε and RSM models except that the discretization technique for the momentum equation is the bounded central differencing scheme. The LES were first used to calculate the transient flows for 1.0 s to reach a statistically stable state, and then for another 0.5 s to obtain statistically steady-state solutions. The time step for LES was adjusted to ensure that the number of iterations for each time step was between five and ten (ANSYS FLUENT 2009).

Pressure Loss Coefficient. Let us use the duct fitting for the diverging and converging flow used by ASHRAE Standard 120, as shown in Figure 1, as an example. The pressure loss coefficient for the duct fittings, C_s, is defined by Equation 1 as the ratio of the total pressure loss across PL-1 and PL-2 to the dynamic pressure at PL-8 for the diverging case or PL-7 for the converging case. The branch loss coefficient, C_b, is defined by Equation 2 as the ratio of the total pressure loss across PL-1 and PL-3 for the diverging case or PL-3 and PL-2 to the dynamic pressure at PL-9 for the converging case.

$$C_s = \frac{\Delta P_{t,1-2}}{P_{d8}}(diverging\,case)\ \textbf{or}\ \frac{\Delta P_{t,1-2}}{P_{d7}}(converging\,case) \tag{3}$$

$$C_b = \frac{\Delta P_{t,1-3}}{P_{d9}}(diverging\,case)\ \textbf{or}\ \frac{\Delta P_{t,3-2}}{P_{d9}}(converging\,case) \tag{4}$$

Where C is the pressure loss coefficient, P is the pressure, and subscripts b is the branch section, c is the common section (section PL-7 in Figure 1(a) and section PL-8 in Figure 1(b)), s is the straight (main) section (section PL-8 in Figure 1(a) and section PL-7 in Figure 1(b)), t is the total; d is the dynamic, and the numbers are for different planes shown in Figure 1. The dynamic pressure at PL-7, PL-8, and PL-9 can be obtained directly in the calculated results as the flow there is fully-developed. However, the total pressure at PL-1, PL-2, and PL-3 could not be directly determined since the flow at these planes is not fully-developed and there normally is significant recirculation in the vicinity of the downstream of the duct fittings. Therefore this study calculated the total pressure loss between PL-7, PL-8, and PL-9, and then minus the on-way resistance by using the Darcy-Weisbach equation to obtain the total pressure loss between PL-1, PL-2, and PL-3. The detailed calculations are shown by Equations (5), (6), and (7), respectively.

$$\Delta P_{t,1-2} = \Delta P_{st,7-8} + (P_{d7} - P_{d8}) - (L_{7-1}\Delta P_{f,7-1} + L_{2-8}\Delta P_{f,2-8}) \tag{5}$$

$$\Delta P_{t,1-3} = \Delta P_{st,7-9} + (P_{d7} - P_{d9}) - (L_{7-1}\Delta P_{f,7-1} + L_{3-9}\Delta P_{f,3-9}) \tag{6}$$

$$\Delta P_{t,3-2} = \Delta P_{st,9-8} + (P_{d9} - P_{d8}) - (L_{9-3}\Delta P_{f,9-3} + L_{2-8}\Delta P_{f,2-8}) \tag{7}$$

where, L is length and subscript st stands for static and f for friction.

As an example, L_{7-1} represents the separation distance between the upstream taps and the entrance plane of the fitting, and $\Delta P_{f,7-1}$ the friction pressure loss per unit length. This friction loss coefficient is calculated by the Darcy-Weisbach equation (Brown 1999), and the related friction factor can be referred to in the Moody diagram (Moody 1944).

Case description

ASHRAE provided two sets of duct fittings for the competition: a flat oval with tee junction as shown in Figure 2(a) and a flat oval with lateral junction in Figure 2(b). Table 1 shows the detailed geometric information. The material of the duct fittings is galvanized steel, and the surface roughness ε of the duct fittings provided by AHSRAE is 0.09 mm (0.0003 ft). By using the duct fitting for the converging and diverging flows, a total of four cases stipulated by the competition were studied:

- Case 1: flat oval straight body with tee junction for converging airflow,
- Case 2: flat oval straight body with tee junction for diverging air flow,
- Case 3: flat oval straight body with lateral junction for converging airflow, and
- Case 4: flat oval straight body with lateral junction for diverging air flow.

Our investigation extended the simulated domain according to the standard lab test apparatus in compliance with ASHRAE Standard 120 as shown in Figure 1, as we believe that any tests should comprise the standard as well. The length of the straight duct in the upstream was 11.5 times that of the inlet hydraulic diameter, and the length of the straight duct in the downstream was 15 times that of the outlet hydraulic diameter. The surface roughness of the straight duct was not provided by ASHRAE and is probably unknown. The inlet velocity ranged between 5.1 ~ 20.3 m/s (1000 ~ 4000 fpm), corresponding to a common section Reynolds number of 85,000 to 500,000. To keep the airflow rate and flow ratios varied over a reasonably wide and realistic range from 0.1 to 0.9, Table 2 shows the inlet boundary conditions and flow ratios used in this study. The inflow turbulence intensity provided was 10% as provided by the ASHRAE.

Results

Since the experimental data of the pressure loss coefficients for the duct fittings were not provided to us before we submitted our simulated results to ASHRAE, this study first validated the CFD models according to the ASHRAE guidelines for using CFD (Chen and Srebric 2002) by using other experimental data from the literature. Then this investigation calculated the pressure loss coefficients for the four cases with the validated CFD model. This section also reported the predicted results compared with the experimental data that were available after we reported the results to ASHRAE.

Validation of the CFD Models for a Similar Case. According to ASHRAE guidelines for validating CFD (Chen and Srebric 2002), we found a flat oval elbow through the literature search, as shown in Figure 3(a). Kulkarni et al. (2009) measured the pressure loss coefficients that can be used to validate the CFD models discussed above. The geometry of the elbow as shown in Figure 3(a) was A × a = 356 × 152 mm (14 × 6 in.). Our simulated domain was also extended according to the standard lab test apparatus in compliance with ASHRAE Standard 120, by connecting the elbow with a straight duct on both ends, as shown in Figure 3(b). Kulkarni et al. (2009) stated that the elbow was constructed using galvanized steel. Since the material of the elbow was the same as that of the two duct fittings used by ASHRAE, the surface roughness ε of the elbow was regarded as 0.09 mm (0.0003 ft), which was provided by ASHRAE. However, the surface roughness of the straight ducts used by Kulkarni et al. (2009) is unknown to us.

This study first examined the grid independence for the three CFD models. The investigation used a mesh generation program, Gambit 2.4.6 (FLUENT 2006), to generate mesh for the elbow. The mesh consisted of structured hexahedron and prism cells as shown in Figure 4 since hexahedral mesh results in fewer cells, while prism mesh is more flexible. Most of the cell sizes were 15 mm, 10 mm, and 8 mm, respectively, for the three meshes used to test the grid dependence. The corresponding number of cells were 0.19 million, 0.61 million, and 1.28 million, respectively. In the tests, the surface relative roughness of the straight duct (ε/D) was assumed to be 0.001, where D is the hydraulic diameter of the duct.

Figure 5 depicts the grid independent study for the elbow with the RSM. The results were the relationship between different airflow rates and pressure losses that were most important for studying the pressure loss for the duct fittings. The case with 15-mm mesh deviated most from the experimental data. The other two mesh sizes gave better results but the discrepancies were still notable between the computed and measured total pressure losses. Nevertheless, the results of the two cases with mesh sizes of 10 and 8 mm were nearly identical. Therefore, a mesh size of 10 mm was considered to be sufficiently good for the RSM. Although not shown here, the 10 mm mesh was also found to be good enough for the standard k-ε model and LES.

Since Figure 5 shows the discrepancies between the calculated and measured pressure loss, this investigation suspected that the surface roughness of the straight ducts could play an important role. Since Kulkarni et al. (2009) did not provide the surface roughness, this study tested its impact on the prediction of the pressure loss by assuming the surface roughness to be 0.01 and 0.001, respectively. Figure 6 shows that the results with a 0.01 surface roughness were in better agreement with the experimental data for the RSM. The same trend could also be seen from the results with the standard k-ε model, but not for the LES. Figure 6 also shows that the standard k-ε model and RSM seemed to perform better than the LES in predicting the pressure loss for this elbow. This was a surprising result as LES is a more advanced model and should perform better than the other two models. Our investigation could not identify the reason.

As Figure 6 shows the strong impact of the surface roughness on the predicted pressure loss, this study investigated its impact further by varying it from 1.0×10^{-5} to 0.1 under a constant inlet velocity of 22.13 m/s (4356.3 fpm), which was a mean value used in the experiment. Figure 7 shows the impact of the surface roughness on the predicted loss coefficient for the three CFD models. The measured loss coefficient at this velocity was 1.446. Clearly, the LES under-predicted the loss coefficient in this range of the surface roughness, which may cover the possible range for the ducts actually used in the experiment. Therefore, LES was not used for further studies. When the surface relative roughness was 5.0×10^{-3}, the standard k-ε model and RSM predicted a peak loss coefficient that was close to the measured one (Kulkarni et al. 2009). Moreover, the predicted loss coefficient by the standard k-ε model was both the largest and the closest to the one measured by Kulkarni et al. (2009).

To further verify the impact of the surface roughness on the pressure loss, this investigation calculated the loss coefficient at different air velocities in the elbow when the surface relative roughnesses of the straight duct were set as 0.002, 0.005, and 0.01, respectively. Figure 8 shows that the predicted loss coefficients with RSM were 1.35, 1.39, and 1.29 and with the standard k-ε model were 1.29, 1.42, and 1.38, respectively. The predicted loss coefficients with both CFD models were within 5% of the measured data

from Kulkarni et al. (2009) when the surface relative roughness of the straight duct was 0.005. Therefore, the RSM and standard k-ε model were applied for further studies shown in the next sub-section.

Prediction of Loss Coefficient for the Tee and Lateral Junctions. Using the same procedure as in the previous sub-section, this study applied the standard k-ε model and RSM in predicting the pressure loss coefficient for the tee and lateral junctions. The inlet boundary conditions were to specify velocity and the outlet boundary conditions were set as pressure for converging conditions and as outflow for diverging conditions. Since the geometry of the tee and lateral junctions is quite different from that of the elbow, this investigation again conducted a grid independence study for the four cases described in the "CASE DESCRIPTION" section, respectively. The procedure of the grid independence study was the same as for the elbow, so it will not be repeated here. The required grid numbers for the four cases were found to be 0.43, 0.53, 0.64, and 0.36 million, respectively.

This investigation used the duct network shown in Figure 1 for studying the pressure loss coefficients of the tee and lateral junctions. The surface roughness of the straight ducts was again unknown. Since the study in the previous sub-section showed a strong impact of the surface roughness in predicting the pressure loss of the elbow, this study assumed that a similar impact would occur for the tee and lateral junctions. In order to estimate the surface roughness, this study first assumed the surface roughnesses to be 0.01 and 0.001, respectively, by using the same procedure as for the elbow. Figure 9 shows the pressure loss coefficients for the four cases under different flow rates at the two surface roughness values. The loss coefficient is a function of the flow ratio (Q_b/Q_c or Q_s/Q_c), where Q_b is the flow rate of the branch section, Q_c the flow rate of the common section, and Q_s the flow rate of the straight (main) section. The loss coefficient is no longer as constant as that of the elbow. For the converging cases, the loss coefficient for the branch increased with the flow rate as the higher flow rate led to a higher resistance. However, the pressure loss coefficient for the main branch in the converging tee junction became smaller when the flow rate increased, as shown in Figure 9(b). For diverging flow, the pressure loss coefficient decreased as the flow rate increased. Therefore, the angle of the junction may have a significant influence on the loss coefficient. Most importantly, the results show again that the roughness played a very important role in predicting the pressure loss coefficients.

Since a similar trend on the surface roughness was observed in the elbow, this study again investigated further the impact of the surface roughness by varying it from 1.0×10^{-5} to 0.15 under one inlet velocity and flow rate ratio as shown in Table 3. Figure 10 shows the predicted loss coefficient with different surface roughnesses for the straight ducts for Case 1. The curve shape in Figure 10 is similar to that in Figure 7 with the two CFD models. The two CFD models again predicted a peak pressure loss coefficient for the main and branch ducts which corresponds to the surface relative roughness of 0.01. In the elbow case, the corresponding surface roughness with the predicted peak loss coefficient by the standard k-ε model was the closest to the measured coefficient by Kulkarni et al. (2009). This study assumed that the surface roughness of 0.01 would lead to the best pressure loss coefficient. In addition, the RSM predicted a higher peak loss coefficient than that of the standard k-ε model, which may indicate that RSM is a better model.

Although not shown here, this study conducted the same tests for the other three cases, and all of them found a peak pressure loss coefficient as summarized in Table 4. Note that the RSM gave a higher peak loss coefficient for Cases 1 and 2, but the standard k-ε model produced a higher coefficient for Cases 3 and 4. Therefore, the surface roughness and turbulence models shown in Table 4 were used for predicting the pressure loss coefficients for the two duct fittings, as requested by ASHRAE.

Figure 11 shows the airflow distributions in the two duct fittings, with converging and diverging flows. All four cases showed a separated region, although some were larger than others. The airflow patterns look very plausible. CFD can easily produce such detailed airflow patterns, but it would be rather complicated to measure them. Such a measurement would need a particle image velocimetry that would cost thousands of dollars.

After submitting the predicted loss coefficients to ASHRAE Project Monitoring Subcommittee 1493, they provided us the corresponding experimental data (ASHRAE PMS-1493, 2011). Figure 12 compares the predicted loss coefficients at different flow ratios with the experimental data. **Please note that the numerical results used in Figure 12 are exactly the same as we submitted to ASHRAE prior to the ASHRAE sending us the experimental data.** In general, this study predicted the pressure loss coefficients with quite good accuracy. Only on a few occasions did the predictions differ from the experimental data by more than 20%, as shown in the figure. The differences were particularly apparent when $Q_b/Q_c \rightarrow 0$ in Figure 12(a), and $Q_s/Q_c \rightarrow 0$ in Figure 12(h). This might be caused by the larger velocity difference between

the branch and main duct when $Q_b/Q_c \rightarrow 0$ or $Q_s/Q_c \rightarrow 0$. At these extreme conditions, the simulation and experiment may both have errors. Since the experimental data also show some irregularities and may contain some errors, it is hard to identify whether the computational results or experimental data are more accurate when there are discrepancies.

ASHRAE Research Project 1493 also requested us to develop the relationship between the loss coefficients and the flow ratios. This investigation found that the loss coefficients C_s and C_b can be expressed as a function of Q_b / Q_c and Q_s / Q_c:

$$C_s = y_0 + A \times e^{R_0 \frac{Q_s}{Q_c}} \textbf{ or } C_b = y_0 + A \times e^{R_0 \frac{Q_b}{Q_c}} \quad (8)$$

where y_0, A and R_0 are constant. Table 5 shows the constant for Equation (8). When the Q_b / Q_c or Q_s / Q_c increases, the second part on the right of Equation (6) will become small and the loss coefficient will approach y_0.

Discussion

In this study, the calculation domain was extended according to the standard lab test apparatus specified by ASHRAE Standard 120. This extension aims to eliminate the influence of the inlet velocity on the pressure distribution. In actual situations, the straight duct may not be that long. The pressure coefficient would vary. CFD models can be used in studying almost all the possible scenarios in practice.

With a certain surface roughness of the straight ducts, the standard k-ε model and RSM could predict peak loss coefficients for the elbow, tee, and lateral junctions. The peak loss coefficients were found to be closest to the measured data in all the cases studied here. The tuned relative roughness was 0.005 or 0.01 and the corresponding absolute surface roughness for the main duct was 0.0026 mm or 0.0051 mm. Comparing with the absolute roughness (0.09 mm) of the duct fittings, there was one order of magnitude difference. We do not know whether this was a coincidence or a true mechanism.

Conclusion

This investigation is part of ASHRAE Research Project 1493, "CFD Shootout Contest – Prediction of Duct Fitting Losses." The study tested different CFD models for predicting the pressure loss coefficient of two duct fittings for converging and diverging flows. The investigation has led to the following conclusions:

- The grid independent studies found that a mesh size of 10 mm was sufficient for the CFD simulations.
- The surface roughness of the straight ducts had a significant influence on the predicted pressure loss coefficient. This investigation found that the predicted loss coefficients varied with different surface roughnesses. The peak coefficients agreed the best with the measured data.
- The performances of the standard k-ε model and RSM were almost identical, and the predicted pressure loss coefficients agreed well with the measured data. LES is an advanced turbulence model, but it failed in predicting the flows in the duct fittings.
- This investigation has developed a procedure on how to use CFD to predict correctly the pressure loss coefficient of a duct fitting. The accuracy of the prediction is generally within 20% of the measured data.

Acknowledgement

The research presented in this paper was financially supported by the National Basic Research Program of China (The 973 Program) through grant No. 2012CB720100.

References

AHSRAE. 2008. *ANSI/AHSRAE Standard 120-2008, Method of testing to determine flow resistance of HVAC ducts and fittings.* Atlanta: American Society of Heating, Air-Conditioning and Refrigeration Engineers, Inc.

ASHRAE PMS-1493. 2011. Private email communications with the CFD experts of ASHRAE Project Monitoring Subcommittee 1493.

Brown, G. 1999. Henry Darcy and his law. http://biosystems.okstate.edu/darcy/index.htm

Chen, Q., and Srebric, J. 2002. A procedure for verification, validation, and reporting of indoor environment CFD analyses. *HVAC&R Research* 8(2): 201-216.

FLUENT. 2006. FLUENT 6.3 Users Guide. Fluent Inc., Lebanon, NH.

FLUENT. 2009. FLUENT 12.0 Documentation. Fluent Inc., Lebanon, NH.

Gan, G., and Riffat, S. 1995. k-factors for HVAC ducts: Numerical and experimental determination. *Building Service Engineering Research and Technology* 16(3):133-139.

Gan, G., and Riffat, S. 1997. Pressure loss characteristics of orifice and perforated plates. *Experimental Thermal and Fluid Science* 14(2):160-165.

Germano, M., Piomelli, U., Moin, P., and Cabot, W. 1996. Dynamic subgrid-scale eddy viscosity model. *In Summer Workshop, Center for Turbulence Research, Stanford, CA.*

Gibson, M., and Launder, B. 1978. Ground effects on pressure fluctuations in the atmospheric boundary layer. *Journal of Fluid Mechanics* 86:491-511.

Kulkarni, D., Khaire, S., and Idem, S. 2009. Measurements of flat oval elbow loss coefficients. *ASHRAE Transactions* 115(1):35-47.

Launder, B., and Spalding, D. 1974. The numerical computation of turbulent flows. *Computer Methods in Applied Mechanics and Energy* 3:269-289.

Mahank, T., and Mumma, S. 1997. Flow Modeling of flat oval ductwork elbows using computational fluid dynamics. *ASHRAE Transactions* 103(2):365-374.

Moody, L. 1944. Friction factors for pipe flow. *Transactions of the ASME* 66(8): 671-684.

Mumma, S., Mahank, T., and Ke, Y. 1997. Close coupled ductwork fitting pressure drop. *HVAC&R Research* 3(2): 158-177.

Mumma, S., Mahank, T., and Ke, Y. 1998. Analytical determination of duct fitting loss-coefficients. *Applied Energy* 61: 229-247.

Shao, L., and Riffat, S. 1995. Accuracy of CFD for predicting pressure losses in HVAC duct fittings. *Applied Energy* 51: 233-248.

Ugursal, A., and Culp, C. 2007. Comparative analysis of CFDΔP vs. measured ΔP for compressed flexible ducts. *ASHRAE Transactions* 113(1): 462-469.

Table 1. Geometry of the Duct Fittings

Nominal Fitting Size, mm (in.) [A × a to C × c (Figure 2)]	Description
787 × 356 to 559 × 254 mm (31 × 14 to 22 × 10 in.)	Tee junction
787 × 356 to 559 × 254 mm (31 × 14 to 22 × 10 in.)	Lateral junction

Table 2. Inlet velocity and flow rate ratios for the four cases

Converging cases						Diverging cases	
Main velocity m/s (fpm)	Branch velocity m/s (fpm)	Q_b/Q_c	Main velocity m/s (fpm)	Branch velocity m/s (fpm)	Q_b/Q_c	Main velocity m/s (fpm)	Q_b/Q_c
20.3 (3996)	5.1(1004)	0.11	11.1 (2185)	20.3 (3996)	0.48	20.3 (3996)	0.1
17.1 (3366)	5.1(1004)	0.13	8.1 (1594)	17.1 (3366)	0.52	20.3 (3996)	0.15
20.3 (3996)	8.1 (1594)	0.17	8.1 (1594)	20.3 (3996)	0.56	20.3 (3996)	0.2
17.1 (3366)	8.1 (1594)	0.19	5.1 (1004)	14.1 (2776)	0.58	20.3 (3996)	0.3
20.3 (3996)	11.1 (2185)	0.22	5.1 (1004)	17.1 (3366)	0.631	17.1 (3366)	0.4
17.1 (3366)	11.1 (2185)	0.25	5.1 (1004)	20.3 (3996)	0.67	14.1 (2776)	0.5
17.1 (3366)	14.1 (2776)	0.29				14.1 (2776)	0.6
11.1 (2185)	11.1 (2185)	0.34				14.1 (2776)	0.7
14.1 (2776)	17.1 (3366)	0.38				11.1 (2185)	0.8
8.1 (1594)	11.1 (2185)	0.41				11.1 (2185)	0.85
5.1 (1004)	8.1 (1594)	0.45				11.1 (2185)	0.9

Q_b - flow rate of the branch section, Q_c - flow rate of the common section.

Table 3 Conditions for testing different surface roughnesses of the straight ducts

Case	1	3	Case	2	4
Main Velocity	11.1 m/s (2185 fpm)	11.1 m/s (2185 fpm)	Main Velocity	14.1 m/s (2776 fpm)	14.1 m/s (2776 fpm)
Branch velocity	8.1 m/s (1595 fpm)	8.1 m/s (1595 fpm)	Q_b / Q_c	0.1	0.2

Q_b - flow rate of the branch section, Q_c - flow rate of the common section

Table 4 The optimal surface roughness of the straight duct and turbulence model identified for the four cases specified by ASHRAE RP-1493

Case	Model	Surface roughness	Case	Model	Surface roughness
1	RSM	0.01	3	Standard k-ε	0.005
2	RSM	0.01	4	Standard k-ε	0.01

Table 5 Parameters for Equation (6)

Item	Parameter	Case 1)	Case 2)	Case 3)	Case 4)
C_b	y_0	1.20	1.46	0.54	0.73
	A	-1.25E+02	1.02E+02	-9.86E+01	1.07E+02
	R_0	-26.52	-15.16	-19.7	-17.63
C_s	y_0	0.32	0.16	0.34	0.30
	A	81.72	139.67	-220.82	174.54
	R_0	-6.56	-19.09	-11.67	-17.40

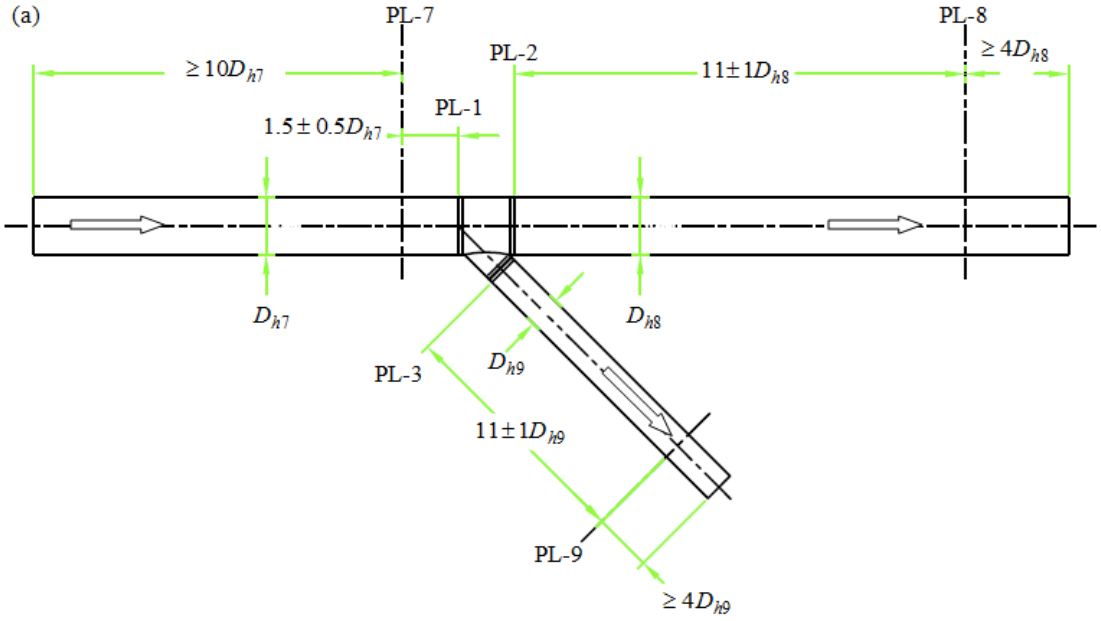

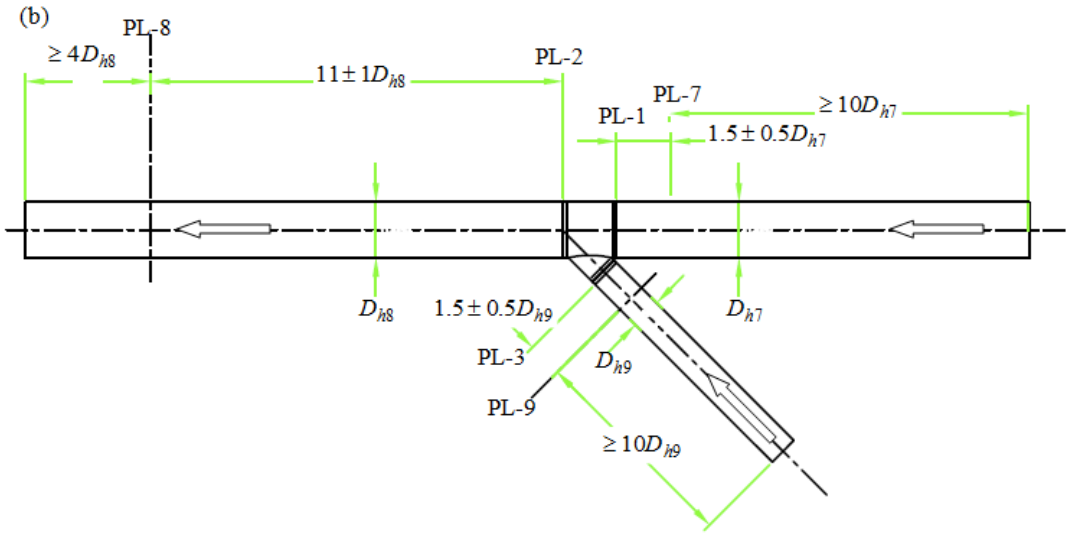

Figure 1 *(a) Diverging and (b) converging airflow test apparatus used by ASHRAE Standard 120*

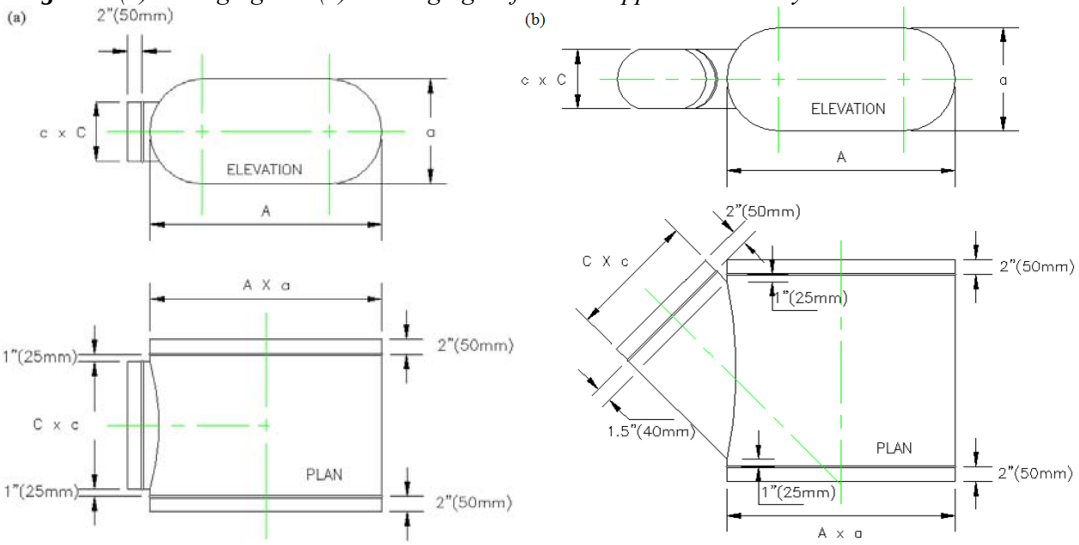

Figure 2 *(a) Flat oval straight body with tee junction and (b) flat oval straight body with lateral junction*

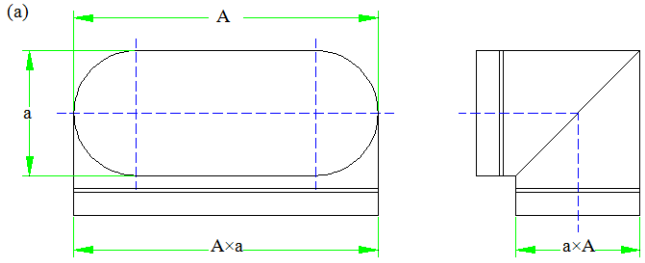

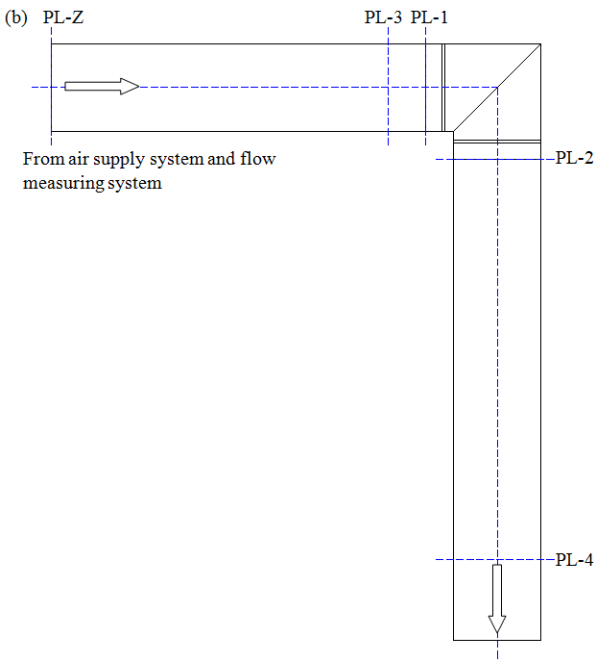

Figure 3 *(a) Mitered 90° easy bend elbow without vanes and (b) its simulation domain*

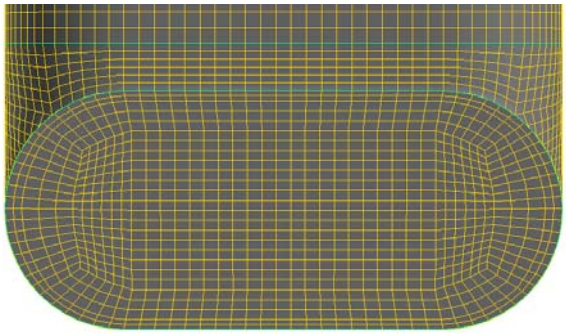

Figure 4 *The cell distribution for the elbow when most cell sizes were 10 mm*

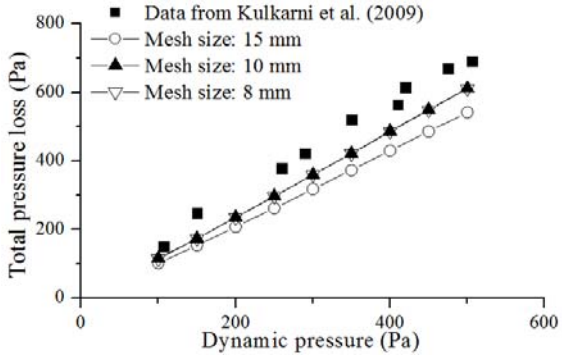

Figure 5 *Grid independence study for the elbow by using the RSM.*

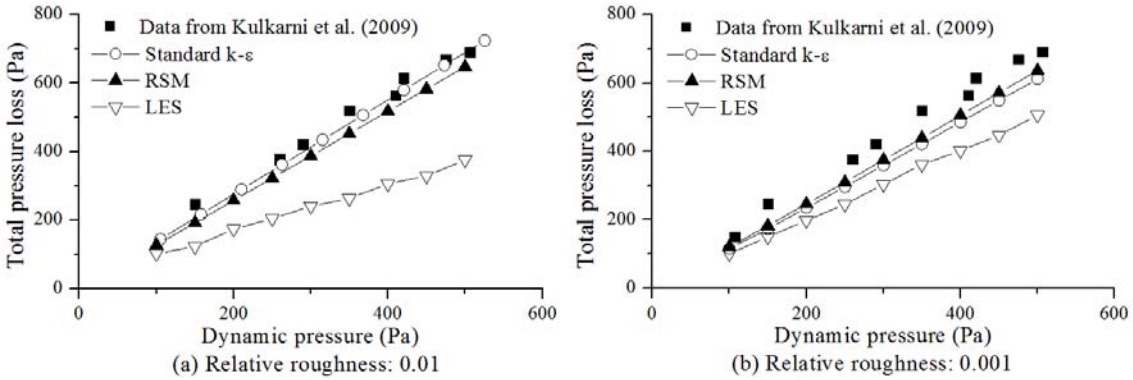

Figure 6 *Predicted pressure loss with different CFD models that had different flow rates at surface relative roughnesses of (a) 0.01 and (b) 0.001*

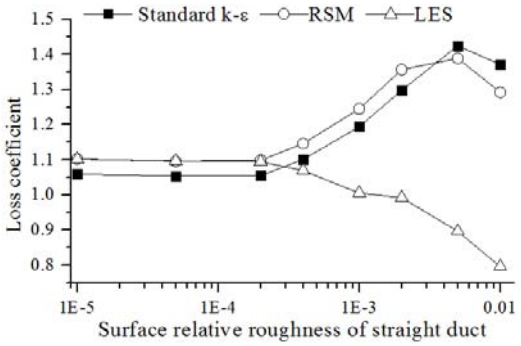

Figure 7 *The loss coefficient calculated with different surface relative roughnesses for an air velocity of 22.13 m/s (4356.3 fpm) in the elbow*

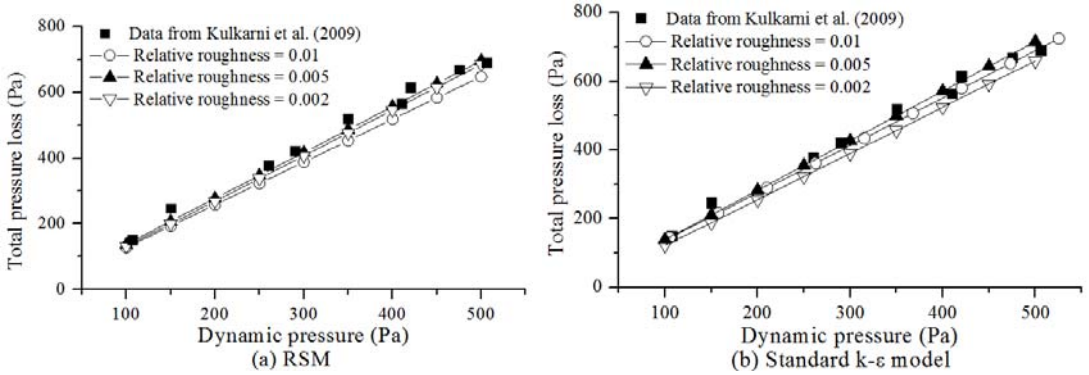

Figure 8 *Comparison of measured pressure loss coefficients for different air velocities with those calculated by (a) RSM and (b) the standard k-ε model under different surface roughnesses*

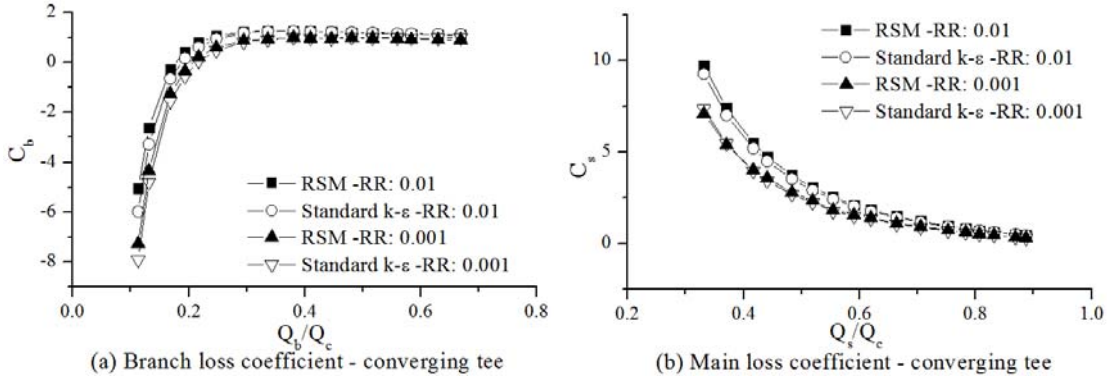

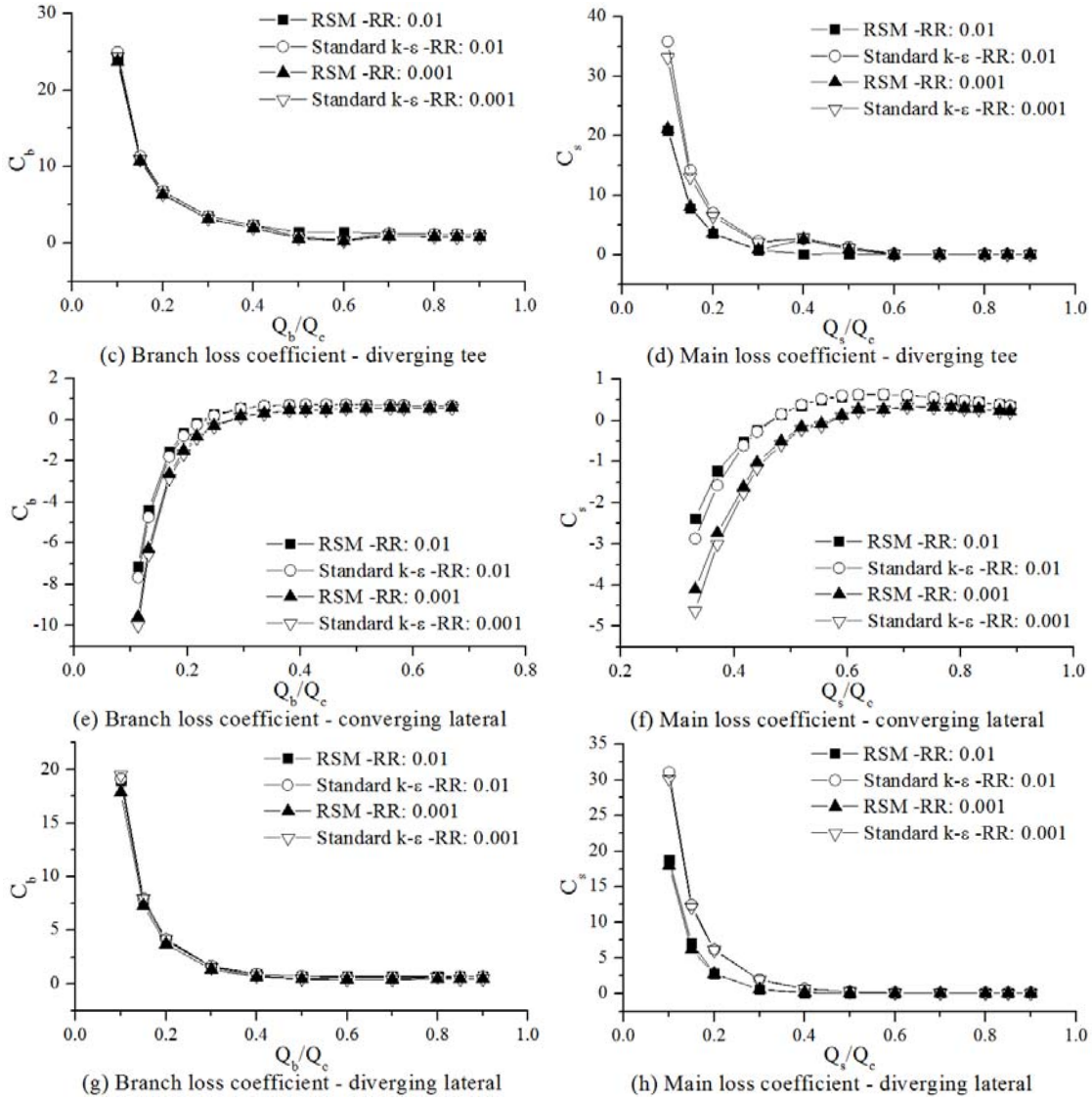

Figure 9 *Predicted pressure loss coefficients by the two CFD models under two different surface relative roughness values for the straight ducts (RR=relative roughness).*

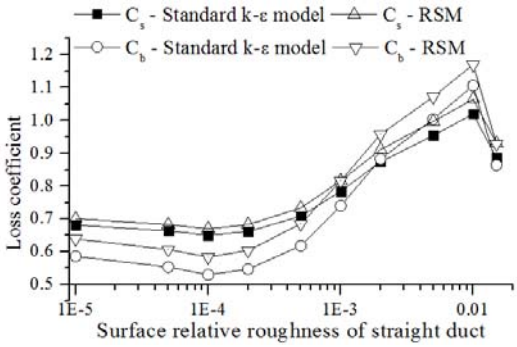

Figure 10 *Predicted loss coefficients with different roughnesses for the straight duct for Case 1.*

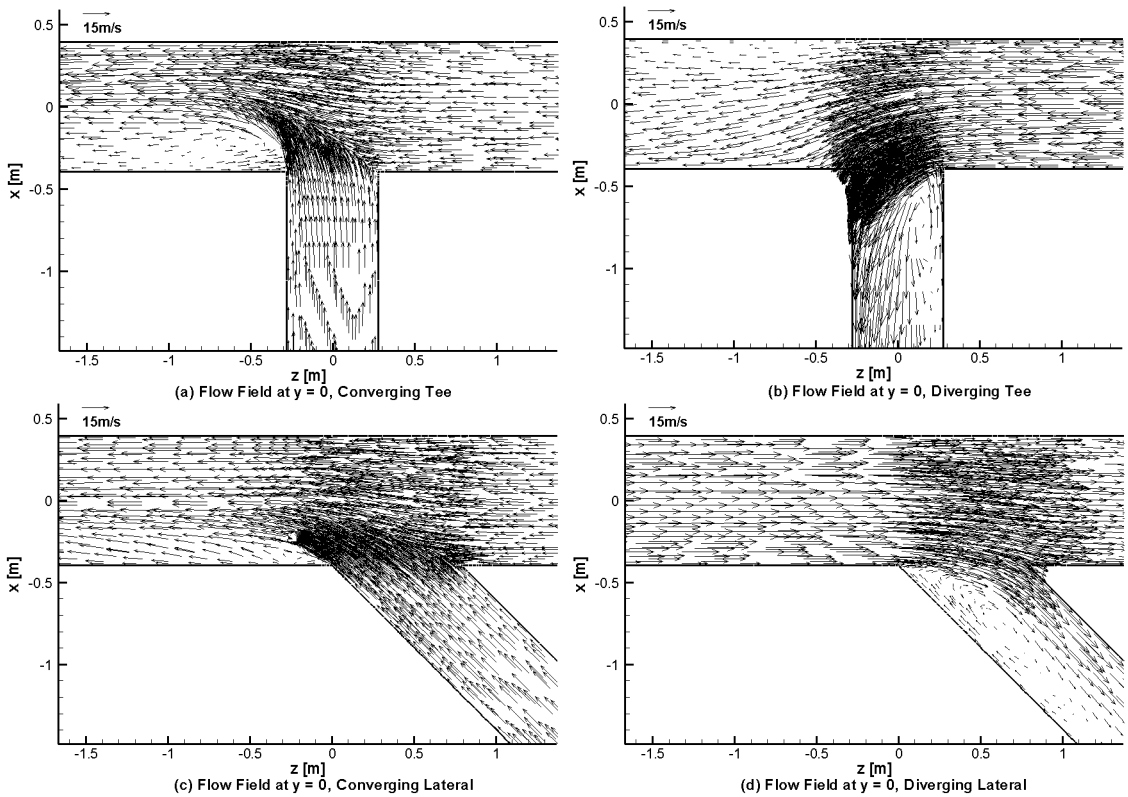

Figure 11 *Airflow patterns at the central cross section for the (a) converging tee, (b) diverging tee, (c) converging lateral, and (d) diverging lateral junctions*

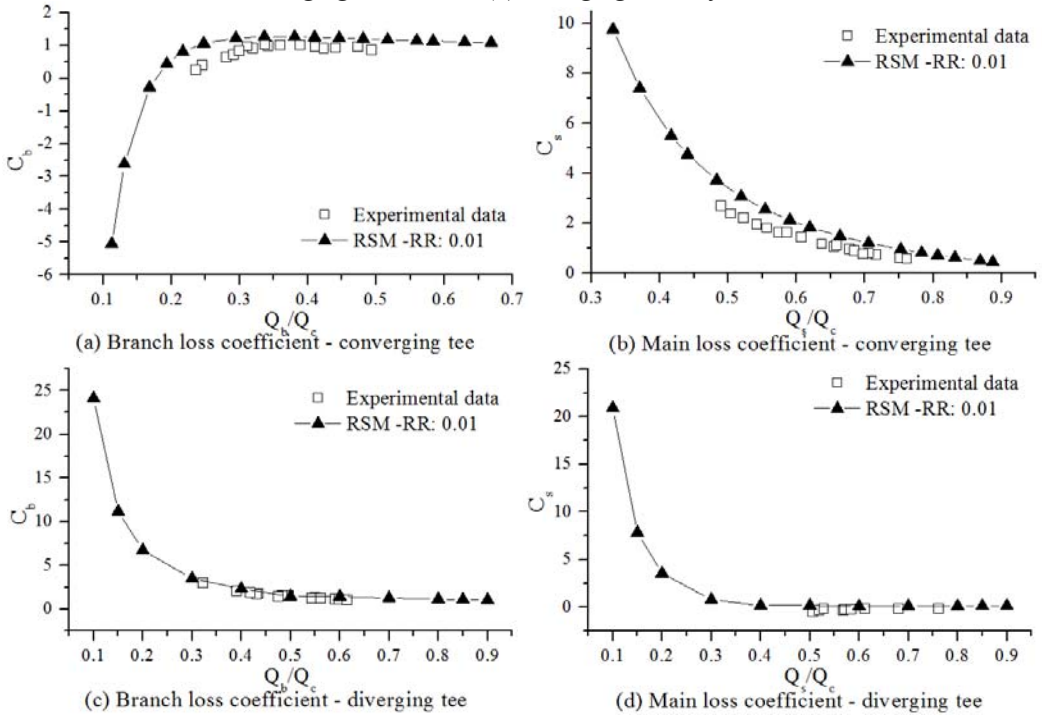

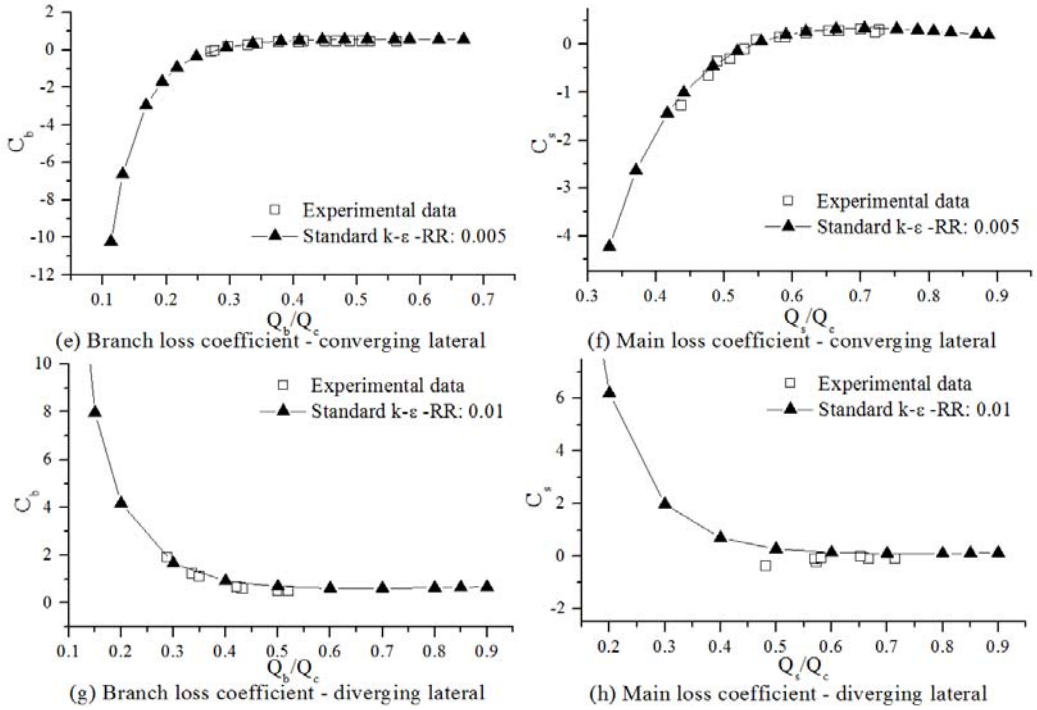

Figure 12 *Comparison of the predicted pressure loss coefficients for different flow rates with the experimental data provided by ASHRAE (RR stands for relative roughness, Experimental data was from ASHRAE)*